Defect detection in aluminium with an eddy currents sensor

E. Ramírez-Pacheco, J. H. Espina-Hernández
SEPI-Electrónica ESIME-Z
Instituto Politécnico Nacional
UPALM, CP 07300 México D.F., México
jhespina@gmail.com

F. Caleyo, J. M. Hallen
DIM-ESIQIE
Instituto Politécnico Nacional
UPALM CP 07738 México D.F., México

Abstract

The purpose of this paper is to present an eddy current testing technique for surface defect detection in conducting materials using a giant magnetoresistive (GMR) sensor. A flat coil is used to produce an alternate magnetic field, which gives rise to eddy currents in the material under test. The GMR sensor with the coil placed on top of it is mounted in a holder, which is moved over the surface of the metal plate using an XY table. Three aluminium plates were used with defects having nominals depths of 2, 4, 6, and 8 mm and widths of 0.6, 1 and 1.4 mm, respectively. The defects were scanned with the sensing axis perpendicular to the defect length. The GMR output voltage depends on the width and depth of the defects. Two parameters extracted from the GMR output voltage signal are obtained and a simple correlation between the defects dimensions and the GMR output voltage is proposed.

Keywords: Eddy currents, giant magnetoresistive sensor, defect detection, defect dimensions, nondestructive evaluation

1. Introduction

Eddy current testing has been widely used in industry in the last decades for nondestructive evaluation (NDE) of materials. Eddy currents (EC) is a common method used for detecting defects such as fatigue cracks, inclusions or voids, and variations in heat treatment, mechanical hardness, impurities and corrosion damages [1].

A time varying magnetic flux density, B, will cause a circulating electric field according to Faraday's law:

$$\nabla \times E = -\frac{\partial B}{\partial t} \tag{1}$$

EC techniques use a coil to generate a changing magnetic field close to the part. The induced EC in the test material absorbs or dissipates energy from the source coil, leading to differences in the flux density. This causes variations in the electrical impedance of the sensor coil, depending on the condition of the test material. The most common EC method is based on the measurement of the electrical impedance of the coil. There are two configurations to measure the impedance, i) using the excitation coil as sensor, or ii) using a pair of differential coils. Inductive sensors are the most commonly used sensors in many measurement systems including EC non-destructive testing. However, the main drawback of induction coils is that their output voltage is proportional to the rate of change of the magnetic flux density rather than to its magnitude, which limits their sensitivity at low frequencies. At high frequencies, EC are confined in a very thin layer. This is the so called skin effect, and as a consequence the magnetic field in the material decreases exponentially. Therefore, detection of deep flaws is difficult with induction coils.

GMR sensors are becomming of great interest nowadays thank to their high and frequency-independent sensitivity to the magnetic field, the small dimensions, the simplicity in use, and low power consumption. GMR sensors detect the component of the magnetic field vector along their sensing axis. In case the field is applied perpendicular to their sensing axis, the effect on the GMR output has negligible effect. Dogaru and Smith [2] proposed a coil - GMR sensor configuration taking advantage of the directional sensitivity of the GMR. A pancake coil was attached to the surface of the GMR sensor, and short cracks at the surface and near the surface were sucessfully detected. Reference [3] presents a real-time nondestructive evaluation of aircraft using GMR-based EC techniques. This work proposed an in-phase quadrature (I/Q) detection, which helps increasing the scanning speed by 50% in comparison to the the magnetooptic imaging technique. References [4] and [5] proposed EC inspection techniques to detect hidden cracks using GMR sensor arrays.

Most of the work in the field of EC techniques are aimed at improving the detection capabilities of the measurement

978-0-7695-4204-1/10 $26.00 © 2010 IEEE
DOI 10.1109/CERMA.2010.91

system. Today industry requirements demand the quantification of the defect dimension rather than simple detection. There exist few works correlating the output signal of the used NDE technique with the actual dimensions of the defect. Ref. [6] is one of the few examples where the authors estimate the defect depth using pulsed eddy current techniques.

The aim of this paper is to correlate the width and depth of large defects of well defined dimensions with the output voltage of the GMR sensor. Mathematical expressions are given to correlate the defect dimensions with the GMR sensor output for the case of scanning the defects with the GMR sensing axis perpendicular to the defect length. A simple procedure to estimate the defects dimensions is proposed taken into consideration the extracted parameters from the GMR output signal.

2. Operation

The EC probe is composed of a flat spiral pancake-type coil with the GMR sensor located on the coil axis as it was proposed in [2]. The probe geometry is shown in Fig. 1, while dimensions of the coil used in the experiments are given in table 1. The excitation coil has two layers with ten turns each. The GMR sensor consists of four resistors in a Weathstone bridge with two as sensing elements and the other two as dummy resistors magnetically shielded by a layer of a material with high magnetic permeability. This layer also acts as flux concentrator for the sensing elements.

The sensing axis of the GMR is coplanar with the inspected surface. The excitation field on the coil axis is perpendicular to the sensing axis of the GMR probe. Therefore, the GMR sensor detects the tangential component of the applied magnetic field (H_t). For a defect-free surface, the output voltage of the GMR sensor will be proportional to H_t. Once the GMR is close to or on top of a defect, the eddy current flow path is altered, which changes H_t due to variation of the mutual inductance between eddy currents and the excitation coil.

Table 1: Geometric parameters of the coil

Inside radius	0.80 mm
Outside radius	2.60 mm
Lenght of the coil	0.36 mm
Number of turns	20
Diameter of the wire	0.18 mm

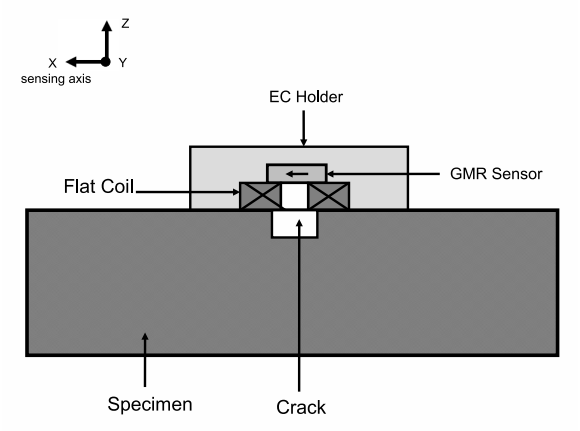

Figure 1: Schematic diagram of the probe assembly with the GMR sensing axis coplanar with the inspected surface.

3. GMR sensor characteristics

A GMR sensor of the type AA002-02 manufactured by NVE was used. Fig. 2 shows the sensor response as measured in the laboratory. The earth magnetic field was not compensated during measurements. The x-axis in Fig. 2 represents the magnetic field in the solenoid where the GMR sensor was placed. Therefore, the small offset voltage in Fig. 2 is due to the earth magnetic field component parallel to the sensing axis of the GMR sensor. The double value near the origin of the sensor output voltage is due to hysteresis, which is a characteristic of this type of sensor. The GMR sensor output is unipolar with a frequency response between dc and 1 MHz. The dc sensitivity of the GMR sensor is 86 mV/mT^{-1} for a dc voltage of 5.15 V supplied to the bridge. The bridge is connected to a set of four nickel-metal hydride batteries with a nominal voltage of 1.2 V each. The sensitivity can be expressed as 17.5 mV/V^{-1}mT^{-1} because the sensor output is linear with the bridge voltage.

4. Experimental setup

Fig. 3 shows the block diagram of the experimental setup for the EC measurements. A sinusoidal voltage signal is selected with an amplitude of 860 mV_{pp} and frequency of 20 kHz in the Agilent 33220A function generator. This signal is fed into a dual audio amplifier LM2879T supplying a current I_{rms} = 780 mA to the excitation coil. The maximum applied magnetic field is about 48 mT in the center of the excitation coil. The penetration depth in aluminium for the applied frequency is approximately 0.6 mm.

The EC probe is scanned over the surface of the aluminium plates in the X direction. The measurements are semi-automatic using the PIC16LF876A to control the

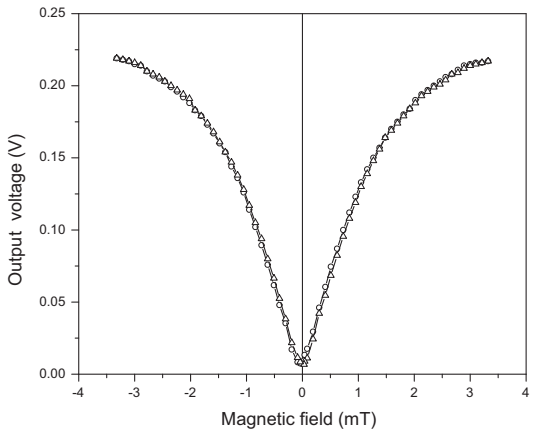

Figure 2: Response of the GMR sensor to a field applied in the direction of its sensing axis.

movement of the XY table. A custom LabVIEW program registers the data from the Agilent digital multimeter 34410A via GPIB interfase. The minimum allowable increment of the XY table in the x-axis was 0.16 mm. The output voltage of the sensor was amplified (G = 10) using an instrumentation amplifier INA118P and low-pass filtered, which helps extracting the dc component of the signal proportional to the defect. The active low-pass filter has a cut-off frequency of 10 Hz. The experiment was conducted with the direction of the GMR sensing axis perpendicular with respect to the defect length.

All defects were scanned ten times and the average value of the extracted parameters were obtained in order to correlate the GMR output voltage with the defects dimensions.

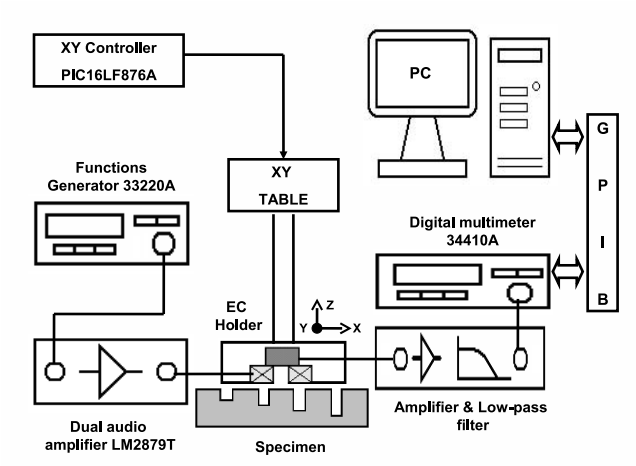

Figure 3: Block diagram of the experimental setup.

Table 2: Actual defects dimensions related to the nominals width (w1, w2, w3) and depths (D1, D2, D3, D4). All values are given in mm.

	D1 = 2 mm	D2 = 4mm	D3 = 6 mm	D4 = 8 mm
w1 = 0.6 mm	2.18; 0.53	3.56; 0.53	6.08; 0.55	7.40; 0.56
w2 = 1.0 mm	1.96; 1.02	4.01; 0.91	5.56; 0.92	7.64; 0.93
w3 = 1.4 mm	1.95; 1.29	4.04; 1.29	6.17; 1.28	7.68; 1.30

Fig. 4 shows the dimensions of the three plates used in this work with their respective machined defects. Each plate has a set of four defects with nominal depths (d) of 2, 4, 6, and 8 mm, and a defect nominal width (w) of 0.6 mm, 1 mm and 1.4 mm, respectively. The defects were mechanically constructed using Cardinal cutting disks of the type $2.5 \times 1/64 \times 1$ inches (100 teeth), $6 \times 1/32 \times 1$ inches (150 teeth) and $2 \times 3/64 \times 5/8$ inches (62 teeth), respectively.

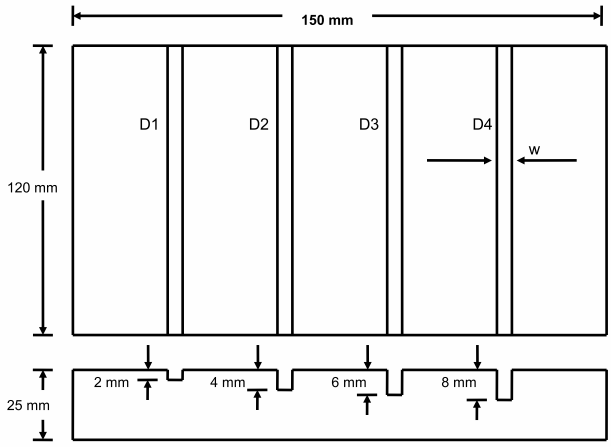

Figure 4: Top and frontal views of the aluminium plates with the defects nominal depths. The nominal widths for three different plates were w1 = 0.6 mm, w2 = 1 mm, and w3 = 1.4 mm.

Table 2 shows the actual values of the defects with nominal widths w1 = 0.6 mm, w2 = 1.0 mm, and w3 = 1.4 mm, and nominal depths D1 = 2 mm, D2 = 4 mm, D3 = 6 mm, and D4 = 8 mm. The width and depth were measured using a Mitutoyo Digital Slide Caliper Model CD-8 CXW and a Starrett Electronic Indicator No-3600 Series, respectively. Both devices have a resolution of 0.01 mm. In table 2 the actual dimensions of each defect is given as pair of values: actual depth; actual width.

5. Results and Discussion

Fig. 5 shows the GMR output voltages of three defects with d = 4 mm and w = 0.6 mm, 1 mm, and 1.4 mm. In case of a defect-free surface the output voltage is about 26 mV, the signal background level in Fig. 5, corresponding to a detected magnetic field of 0.3 mT as obtained from the sensor characteristic of Fig. 2. A magnetic finite elements simulation using the freeware FEEM [7] was performed to obtain the tangential component (H_t) of the applied field in the active region of the GMR sensor. The maximum value of H_t was about 0.25 mT, which supports the experimental results shown in Fig. 5.

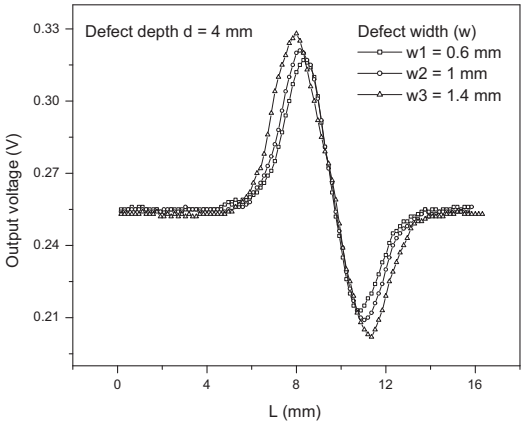

Figure 5: GMR output signals for defects with d = 4 mm and widths of 0.7 mm, 1mm and 1.4 mm. The GMR sensing axis is perpendicular to defect length.

The maximum amplitude of the GMR output voltage in Fig. 5 depends on both dimensions: the depth and width of the three scanned defects. The three signals are from three defects having the same depth of 4 mm and with widths of 0.6 mm, 1 mm and 1.4 mm.

Fig. 6 shows how the parameters i) the voltage difference between peaks (DV), and ii) the difference in position of the peaks (DX) were defined in order to obtain a simple correlation between the GMR output voltage and the defect dimensions for the case of scanning the defect with the GMR sensing axis perpendicular to the defect length. DV is defined as the voltage difference between the maximum and the minimum values of the output signal, and DX is defined as the difference in position, expressed in mm, between them.

It was shown in Fig. 5 that the output voltage maximum value depends on both dimensions. Therefore, a clear correlation between the GMR output voltage and the defect dimensions can be obtained by first estimating the width and later the depth.

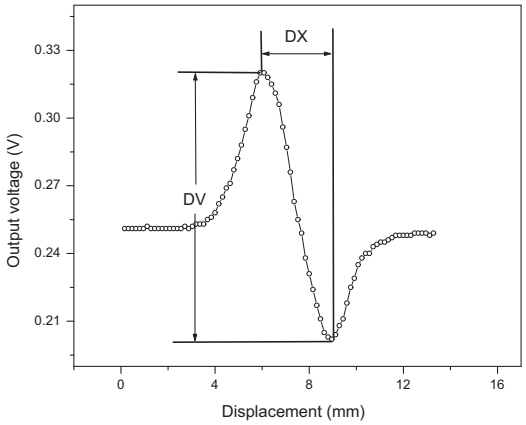

Figure 6: Definition of the parameters DV and DX of the output voltage in the case of scanning the defect with the GMR sensing axis perpendicular to the defect length.

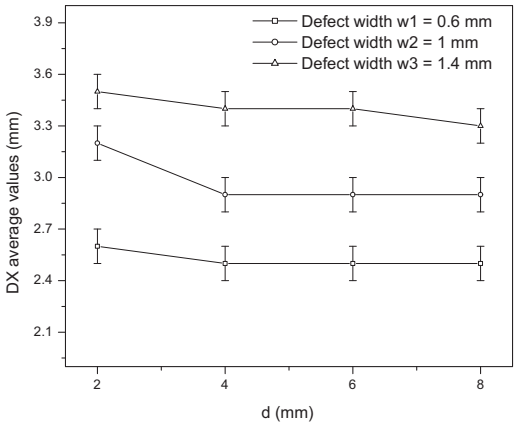

Figure 7: DX average values for each nominal width as a function of the defect depth.

Fig. 7 shows the DX average values of the studied defects. Each plate has four defects with one nominal width and four different nominal depths. It is clearly seem in Fig. 7 that DX shows almost a linear behavior as a function of the defect depth. The DX value related to the defect with w = 1 mm and d = 2 mm is bigger than the respective values for the defects with nominal depths of 4, 6, and 8 mm. From table 2, the actual width of this defect is 1.02 mm, and for the other three defects is 0.91, 0.92, and 0.93 mm, respectively. The width difference of 0.1 mm between the first defect and the mean value of the other three defects in-

fluences the DX differences for the same nominal width. It is worth noting the good resolution of the proposed parameter in order to estimate the actual width of the defect. The DX value can be considered as constant for a given width. In Fig. 7 we can see that there is no overlapping between any two points with their standard deviation. Therefore, it is valid to consider that DX is constant for a given width.

Fig. 8 shows the experimental values of DX and the corresponding linear fit function. In this case, each average value was obtained from all measurements taken from defects with the same nominal width of each aluminium plate. The defect width can be estimated using the linear fit function given in Fig. 8. Therefore, the DX parameter extracted from the GMR output voltage can be used to estimate the defect nominal width.

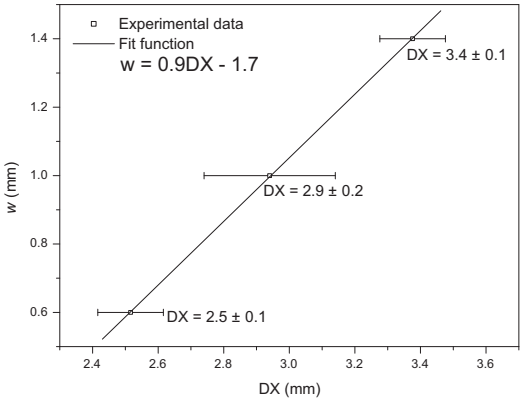

Figure 8: DX average values and the corresponding linear function.

After estimating the width of the scanned defect, the defect depth can be estimated by using the DV parameter extracted from the GMR output voltage.

Fig. 9 shows the DV average values and their respective fit functions for the defects with nominal widths w1 = 0.6 mm, w2 = 1 mm and w3 = 1.4 mm, respectively. The fit function is:

$$DV = a(1 - f^d) \tag{2}$$

where a is a fitting parameter, f is the filling factor of the excitation coil, and d is the defect nominal depth. The coil filling factor is defined as [8]:

$$f = \frac{d_{out} - d_{in}}{d_{in} + d_{out}} \tag{3}$$

where d_{out} and d_{in} are the coil outer and inner diameters, respectively. For the excitation coil used here f = 0.533.

Table 3 shows the fitting parameters using equation 3 for each nominal width. The coil filling factor f was kept constant.

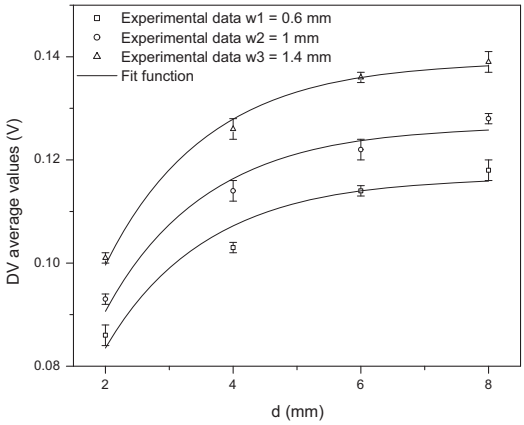

Figure 9: DV average values and the corresponding fit function.

Table 3: Fitting parameters of the experimental values of DV.

Fitting parameters	w1 = 0.6 mm	w2 = 1 mm	w3 = 1.4 mm
a	0.12	0.13	0.14
f	0.533	0.533	0.533
$\chi^2(x10^{-6})$	9.5	6.4	2.1
R^2	0.95	0.97	0.99

According to the results presented in Fig. 9, equation 2 is a good approximation in order to estimate the defect depth once the width has been obtained. The main drawback of the proposed fit function is that DV is the dependant variable. Therefore a straightforward depth estimation is not possible to achieve. Nevertheless, the proposed fit function is rather simple and gives a relationship between a physical parameter of the excitation coil, the proposed extracted parameter DV from the GMR output voltage and the defect nominal depth.

6. Conclusions

An experimental system using eddy current techniques with a GMR sensor was developed. A set of mechanical defects were built in three different plates with four nominal depths (2, 4, 6, and 8 mm) and three nominal widths (0.6,1 and 1.4 mm), respectively. The GMR output voltage is dependent on the defect width and depth when the sensing axis was perpendicular to the defect length. Two parameters are obtained from the GMR voltage voltage, DX and DV. DX and DV help correlating the GMR signal with the actual defect dimensions and can be used to estimate the de-

fects studied dimensions. DX depends only on the defects width and DV is dependant from both defects dimensions. A simple procedure is proposed where the first step is to estimate the width and later the defect depth. The defect depth is estimated depending on the estimated width, and the corresponding function is selected. The proposed fit function gives a relationship between the DV parameter and the defect depth and the filling factor of the excitation coil. It is necessary to propose a function where the depth estimation is straightforward. There is an outgoing investigation where a broader range of widths and depths will be studied.

7. Acknowledgment

This work was partially supported by the projects IPN-SIP-20101027. E. R-P thanks CONACyT and PIFI-IPN for the scholarships.

References

[1] David C. Jiles, *Introduction to the Principles of Materials Evaluation*. CRC Press, Taylor & Francis Groups, 2008, pp. 147-161.

[2] T. Dogaru and S. T. Smith, "Giant magnetoresistance-based eddy-current sensor" *IEEE Trans. Magn.*, vol. 37, no. 5, pp. 3831-3838, 2001.

[3] N. V. Nair, V. R. Melapudi, H. R. Jimenez, Xin Liu, *et al.*, "A GMR-based eddy current system for NDE of aircraft structures" *IEEE Trans. Magn.*, vol. 42, no. 10, pp. 3312-3314, 2006.

[4] F. Vacher, C. Gilles-Pascaud, *et al.*, "Non destructive testing with GMR magnetic sensor arrays", presented at the ECNDT 2006, Berlin, Germany. Available: http://www.ndt.net/article/ecndt2006/doc/Tu.4.4.2.pdf.

[5] A. Yashan, W. Bisle, and T. Meier, "Inspection of hidden defects in metal-metal joints of aircraft structures using eddy current technique with GMR sensor array", presented at the ECNDT 2006, Berlin, Germany. Available: http://www.ndt.net/article/ecndt2006/doc/Tu.4.4.4.pdf.

[6] I. Zainal Abidin, C. Mandache, G. Y. Tian, and Yong Li, "Defect depth estimation using pulsed eddy current with varied pulse width excitation", *Insight*, vol. 51, no. 2, 69-72, 2009.

[7] *Finite element method magnetics, Version 4.0, User Manual*. Available http://femm.foster-miller,net/

[8] S. Mohan Sunderarajan, Maria del Mar Hershenson, P. Boyd, and H. Lee Thomas, "Simple accurate expression for planar spiral inductance", IEEE J. of solid-state circuits, 34(10):1419-1424,1999.